

VIP **Gold Nanoclusters** Very Important Paper

 Deutsche Ausgabe: DOI: 10.1002/ange.201813426
 Internationale Ausgabe: DOI: 10.1002/anie.201813426

Fcc versus Non-fcc Structural Isomerism of Gold Nanoparticles with Kernel Atom Packing Dependent Photoluminescence

 Shengli Zhuang⁺, Lingwen Liao⁺, Jinyun Yuan, Nan Xia, Yan Zhao, Chengming Wang, Zibao Gan, Nan Yan, Lizhong He, Jin Li, Haiteng Deng, Zhaoyong Guan, Jinlong Yang, and Zhikun Wu*

Abstract: Structural isomerism allows the correlation between structures and properties to be investigated. Unfortunately, the structural isomers of metal nanoparticles are rare and genuine structural isomerism with distinctly different kernel atom packing (e.g., face-centered cubic (fcc) vs. non-fcc) has not been reported until now. Herein we introduce a novel ion-induction method to synthesize a unique gold nanocluster with a twist mirror symmetry structure. The as-synthesized nanocluster has the same composition but different kernel atom packing to an existing gold nanocluster $Au_{42}(TBBT)_{26}$ ($TBBT = 4\text{-tert-butylbenzenethiolate}$). The fcc-structured $Au_{42}(TBBT)_{26}$ nanocluster shows more enhanced photoluminescence than the non-fcc-structured $Au_{42}(TBBT)_{26}$ nanocluster, indicating that the fcc-structure is more beneficial for emission than the non-fcc structure. This idea was supported by comparison of the emission intensity of another three pairs of gold nanoclusters with similar compositions and sizes but with different kernel atom packings (fcc vs. non-fcc).

Structural isomerism is an important concept in organic chemistry and has been heavily investigated theoretically for clusters.^[1] Recently this important concept has been studied in the liquid/solid phase nanoparticle field, providing excellent opportunities for understanding the correlation between structure and property in depth.^[2] Metal nanoclusters,^[3] as ultrasmall nanoparticles, are ideal materials to study the structural isomerism at nanoscale because their compositions^[4] and structures^[5] can be precisely determined with the development of characterization techniques such as electrospray ionization mass spectrometry (ESI-MS)^[4c,6] and X-ray crystallography (XC).^[5a] However, only a single pair of genuine structural isomers in liquid/solid phase has been



reported until now,^[2a] although several quasi-structural isomers have been claimed.^[2b-d] Thiolated metal nanoclusters generally consist of pure metal kernels and mixed metal-ligand staple motifs;^[3d,e] recently, it has been revealed that fcc-structured kernels are not an exclusive feature of nanocrystals but are possessed by some nanoclusters as well.^[2d,4e,7] However, the only two structural isomers of metal nanoparticles both possess non-fcc-structured kernels.^[2a] It is questionable whether it is possible to obtain structural isomers in which one has non-fcc and the other has fcc kernel atom packing, given that ligands generally influence the kernel atom packing. For instance, phenylethanethiolated gold nanoclusters always exhibit non-fcc kernel atom packing,^[5b,c,8] while 4-tert-butylbenzenethiolated gold nanoclusters generally have fcc packing.^[7a-f,b]

Metal nanocluster photoluminescence is another phenomenon that has attracted interest not only for fundamental scientific research but also for practical applications.^[3c] However, even the fundamental question regarding the influence of kernel atom packing on metal nanocluster photoluminescence is still unanswered. Because a multitude of factors impact metal nanocluster photoluminescence, such as nanocluster's aggregation,^[9] ligand choice^[10] and Au/SR atomic ratio,^[11] it is necessary to keep these characteristics consistent in order to probe the impact of kernel atom packing. Structural isomers with different metal atom packing (fcc vs. non-fcc) serve as ideal materials for this kind of investigation. With this motivation in mind, we report the successful synthesis of such structural isomers and an investigation of their photoluminescence comparison, which is detailed below.

[*] Dr. S. Zhuang,^[+] Dr. L. Liao,^[+] Dr. N. Xia, Y. Zhao, Dr. Z. Gan, Dr. N. Yan, L. He, Prof. Dr. Z. Wu
 Key Laboratory of Materials Physics, Anhui Key Laboratory of Nanomaterials and Nanotechnology, CAS Center for Excellence in Nanoscience, Institute of Solid State Physics, Chinese Academy of Sciences
 Hefei 230031 (P. R. China)
 and
 Institute of Physical Science and Information Technology, Anhui University
 Hefei, Anhui 230601 (P. R. China)
 E-mail: zkwu@issp.ac.cn
 Dr. J. Yuan, Prof. Dr. C. Wang, Prof. Dr. J. Yang
 Hefei National Laboratory for Physical Sciences at the Microscale, University of Science and Technology of China
 Hefei, Anhui 230026 (P. R. China)

Prof. Dr. J. Li
 Tsinghua University-Peking University Joint Center for Life Sciences, School of Life Sciences, Tsinghua University
 Beijing 100084 (P. R. China)
 Prof. Dr. H. Deng
 MOE Key Laboratory of Bioinformatics, School of Life Sciences, Tsinghua University
 Beijing 100084 (P. R. China)
 Dr. Z. Guan
 Center for Multidimensional Carbon Materials, Institute for Basic Science (IBS)
 Ulsan 44919 (Republic of Korea)

[+] These authors contributed equally to this work.

 Supporting information and the ORCID identification number(s) for the author(s) of this article can be found under:
 <https://doi.org/10.1002/anie.201813426>

4-*tert*-butylbenzenethiol (TBBTH) was chosen as the protecting ligand because a series of fcc-structured gold nanoclusters had been reported using this ligand, including $\text{Au}_{28}(\text{TBBT})_{20}$,^[7b] $\text{Au}_{36}(\text{TBBT})_{24}$,^[7a] $\text{Au}_{42}(\text{TBBT})_{26}$,^[7g] $\text{Au}_{44}(\text{TBBT})_{28}$,^[7d] $\text{Au}_{52}(\text{TBBT})_{32}$ ^[7c] and $\text{Au}_{92}(\text{TBBT})_{44}$.^[7e,f] Medium-sized gold nanoclusters (Au_n , $40 < n < 100$) with non-fcc structures were targeted in this synthesis due to the ease of crystallization compared to that of larger gold nanoclusters and because genuine structural isomers of this size had not yet been reported. We successfully synthesized a non-fcc-structured $\text{Au}_{42}(\text{TBBT})_{26}$ nanocluster (abbreviated $\text{Au}_{42\text{N}}$), which is the structural isomer of the existing fcc-structured $\text{Au}_{42}(\text{TBBT})_{26}$ (abbreviated $\text{Au}_{42\text{F}}$).^[7h] In the synthesis, a foreign cation, cadmium, is necessary, that is, without the addition of Cd, the same product cannot be obtained. The addition of Cd may influence the kinetics and thermodynamics in the producing of $\text{Au}_{42\text{N}}$ nanoclusters by, for example, forming some unstable Au/Cd intermediates, by tuning the reducing ability of NaBH_4 , or by influencing the etching rate of thiol.^[12] However, the detailed mechanisms need to be pursued in the future. Such a synthesis method can be dubbed an “ion-induction” approach in which ions are added into the reaction mixture to induce the formation of the special product(s). Note that such a synthetic method has not been previously reported. Details regarding the synthesis are provided in the Supporting Information. The fcc-structured $\text{Au}_{42\text{F}}$ nanoclusters were synthesized by our previous method.^[7h] Note that, $\text{Au}_{42\text{N}}$ and $\text{Au}_{42\text{F}}$ nanoclusters do not coexist in the given reaction conditions and it is observed that the producing of $\text{Au}_{42\text{N}}$ and $\text{Au}_{42\text{F}}$ is sensitive to both kinetic and thermodynamic parameters (e.g. time, temperature, solvent, Au salt/thiol molar ratio, etc.). In other words, the two isomers are difficult to obtain under alternative conditions, which indicates that the underlying mechanisms to produce one type of cluster over another can be attributed to kinetic control and thermodynamic selection as reported previously.^[12a]

The two structural isomers were characterized by UV/vis/NIR spectroscopy in dichloromethane and electrospray ionization mass spectrometry (ESI-MS) as shown in Figure 1. The absorption spectrum of $\text{Au}_{42\text{N}}$ has two prominent peaks at 365 and 867 nm and three humps at 396, 477 and 619 nm (see Figure 1 a), respectively; while $\text{Au}_{42\text{F}}$ has several weak humps at 400, 440, 490 and 636 nm (see Figure 1 c), respectively. These distinct optical features illustrate the structure difference between the two abovementioned nanoclusters. ESI-MS was applied to determine the formula of the two nanoclusters. To assist the ionization, cesium acetate (CsOAc) was added to the nanocluster solution to form positively charged adducts. A dominant peak centered at m/z 6418.06, corresponding to $[\text{Au}_{42}(\text{TBBT})_{26} + 2\text{Cs}]^{2+}$ (calculated: m/z 6418.17, deviation: m/z 0.11), was observed in the mass spectrum of $\text{Au}_{42\text{N}}$ (Figure 1 b), and a similar peak centered at m/z 6418.32 was also observed in the spectrum of $\text{Au}_{42\text{F}}$ (Figure 1 d), demonstrating that the two nanoclusters have the same formula $\text{Au}_{42}(\text{TBBT})_{26}$. X-ray crystallography (XC) analyses further confirmed the two nanoclusters being structural isomers.

As shown in Figure 2 a, $\text{Au}_{42\text{N}}$ contains a non-fcc Au_{26} kernel that can be split into three units: upper, middle and

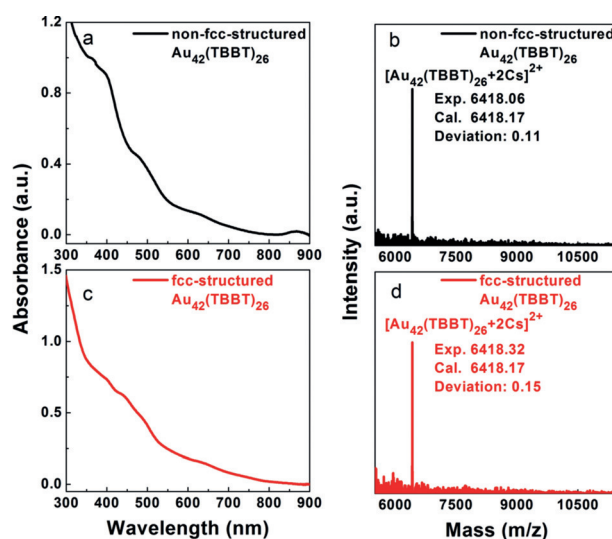


Figure 1. The UV/Vis/NIR absorption spectra and ESI-MS of $\text{Au}_{42\text{N}}$ (a,b) and $\text{Au}_{42\text{F}}$ (c,d).

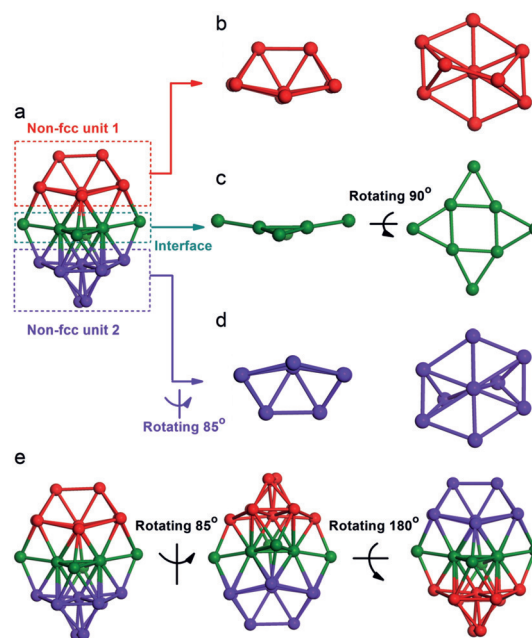


Figure 2. The kernel structure of $\text{Au}_{42\text{N}}\text{-Au}_{26}$ kernel (a), the top and side view of non-fcc unit 1 (b), interface (c) and non-fcc unit 2 (d), and the rotating operation of Au_{26} kernel (e). Red, green, and purple = Au, see text for details. For clarity, all the C and H atoms are omitted.

bottom. As illustrated in Figure 2, both the upper and bottom units are composed of 9 gold atoms, colored red and purple, respectively, and the middle unit has eight gold atoms forming a concave quadrilateral interface, colored green in Figure 2. Interestingly, the Au_{26} kernel is twisted when viewed along the longitudinal axis direction. To illustrate this twisting clearly, the bottom non-fcc-structured Au_9 unit is virtually rotated by about 85° counterclockwise along the longitudinal axis; then, it can be found that the upper and bottom Au_9 units have mirror symmetry as seen in Figure 2 b,d. Similarly, when the Au_{26} kernel is first rotated by around 85° counterclockwise

along the longitudinal axis and then rotated by 180° along the horizontal axis of the kernel, the resulting kernel conformation is the same as the original one (Figure 2e). Note that the two Au₉ units do not form a traditional twin crystal due to their separation by a special Au₈ interface (see Figure 2a), but such a structure is surprising and to our knowledge was not previously reported. In contrast, Au_{42F} contains a fcc-structured Au₂₆ kernel (see Figure S1 in the Supporting Information, and the structure details were illustrated in our previous work).^[7g] Clearly, the two Au₄₂ nanoclusters have distinctly different kernel atom packing (non-fcc vs. fcc).

The Au₂₆ kernel of Au_{42N} is capped by several motifs including four Au₃(TBBT)₄, four Au(TBBT)₂ and two TBBT units (see Figure 3). Specifically, four Au₃(TBBT)₄ units form

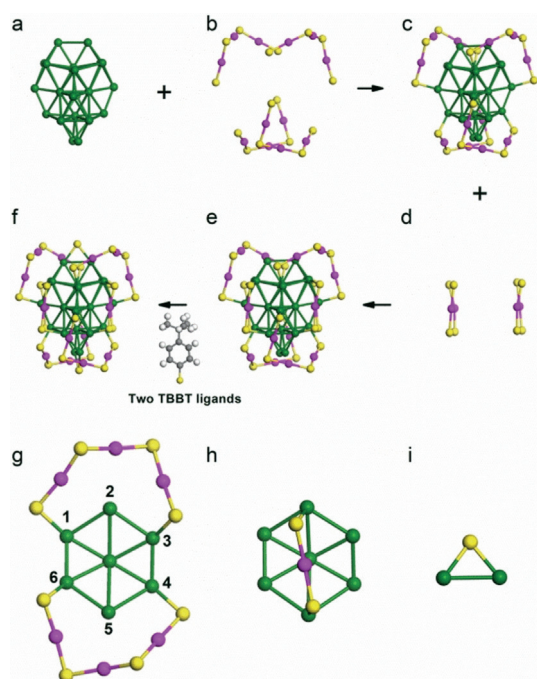


Figure 3. The staple structure of Au_{42N}. The Au₂₆ kernel (a), four Au₃(TBBT)₄ units (b), Au₃₈(TBBT)₁₆ fragment (c), four Au(TBBT)₂ units (d), Au₄₂(TBBT)₂₄ fragment (e), total structure of non-fcc Au₄₂(TBBT)₂₆ (f), the configuration of Au₃(TBBT)₄ (g) and Au(TBBT)₂ (h) staple on the Au₇ facet of the kernel, and the configuration of a single TBBT ligand on the kernel (i). Color label: Magenta and green = Au; yellow = S. For clarity, all the C and H atoms are all omitted.

eight Au_{kernel}-S_{staple} bonds on the surface of the Au₂₆ kernel (Figure 3a–c), four Au(TBBT)₂ units form eight Au_{kernel}-S_{staple} bonds on the waist of the Au₂₆ kernel (Figure 3d,e), and two TBBT ligands contribute to four Au_{kernel}-S_{staple} bonds (see Figure 3f). Figure 3g depicts an enlarged image of four Au_{kernel}-S_{staple} bonds (average bond length: 2.376 Å) formed by the kernel capping from two Au₃(TBBT)₄ units; for an enlarged image showing two Au_{kernel}-S_{staple} bonds (average bond length: 2.376 Å) formed by the kernel capping of one Au(TBBT)₂, see Figure 3h. In contrast, the staple structure of Au_{42F} which was also illustrated in our previous work^[7h] is shown in Figure S2.

As mentioned above, the photoluminescence of metal nanoclusters is influenced by multiple factors,^[9–11] therefore the isolation of structural isomers with distinctly different kernel atom packing provides an excellent opportunity to investigate the kernel atom packing influence on the photoluminescence. There are very few reports regarding photoluminescent gold nanoparticles with fcc-structures (the nanoparticles with photoluminescent ligands are not considered herein); thus, it is anticipated that the fcc structure may be not beneficial to the emission.^[11b] However, our experiments illustrated that Au_{42F} has stronger emission than that of Au_{42N} (the photoluminescence quantum yield of Au_{42F} is about twice as high as that of Au_{42N}, see Figure S3a,b), indicating that the fcc structure does not actually inhibit the emission compared with the non-fcc structure. The density function theory (DFT) calculation reveals that the charge states of total 42 Au atoms (26 ligands) in Au_{42N} and Au_{42F} are +2.678 (–2.678) and +2.898 (–2.898), respectively (Figure S4), which indicates that the kernel atom packing influences the charge distribution between the metal atoms and ligands. The more positive charge state in the metal part (or more negative charge state in the organic part) benefits the charge transfer from ligands to metal part via Au–S bond,^[10] thus triggering more extensive photoluminescence, which provides theoretical interpretation for the fact that fcc-structured Au₄₂ has stronger photoluminescence than non-fcc structured Au₄₂ nanocluster.

We further compared the photoluminescence intensity of another three pairs of gold nanoclusters with similar compositions (sizes) but different kernel atom packings (Figure S5): non-fcc-structured Au₄₄(TBBT)₂₆^[13] versus fcc-structured Au₄₄(TBBT)₂₈,^[7d] non-fcc-structured Au₃₈(2,4-DMBT)₂₄ (2,4-DMBT = 2,4-dimethylbenzenethiolate) versus fcc-structured Au₃₄(2,4-DMBT)₂₂ and non-fcc-structured Au₄₈(TBBT)₂₈^[13] versus fcc-structured Au₅₂(TBBT)₃₂,^[7c] respectively (see Figure S3c–h). Note that non-fcc-structured Au₃₈(2,4-DMBT)₂₄ (see Figure S6a) and fcc-structured Au₃₄(2,4-DMBT)₂₂ (see Figure S6c) are newly synthesized in this work and their structures are similar with previously reported Au₃₈(PET)₂₄ (PET = phenylethanethiolate)^[8] (see Figure S6b) and Au₃₄(CHT)₂₂ (CHT = cyclohexanethiolate (see Figure S6d),^[4e] respectively, without considering the ligand difference (for the comparison of their structures, see Figure S6). For the photoluminescence quantum yield calculation method, the sample concentrations (Table S1) and the cluster extinction coefficients (Figures S7–15), see the supporting information.

The experimental results (see Figure S3) show that in all cases fcc-structured gold nanoclusters have stronger photoluminescence than non-fcc structured gold nanoclusters with similar compositions and sizes, demonstrating that the observation of photoluminescence difference between Au_{42F} and Au_{42N} is not an exclusive case and supporting the hypothesis that the fcc structure might be more beneficial to the photoluminescence than the non-fcc structure.

In summary, our work has shown: 1) a novel synthesis method for metal nanoclusters; 2) three novel nanoclusters (non-fcc Au₄₂(TBBT)₂₆, Au₃₄(2,4-DMBT)₂₂, and Au₃₈(2,4-DMBT)₂₄) were synthesized and characterized with atomic precision; 3) the twist mirror symmetry structure was first observed in metal nanoclusters; 4) for the first time, genuine

structural isomers with distinctly different kernel atom packing (fcc vs. non-fcc) was obtained; and 5) kernel atom packing-dependent photoluminescence was observed for the first time. It is expected that this work will stimulate more research on structural isomerism at the nanoscale and structure–property relationships.

Acknowledgements

We would like to thank National Natural Science Foundation of China (Nos. 21771186, 21222301, 21688102, 21573212, 51502299, 21603234, 21701179, 21171170, 21829501 and 21528303), Key Program of 13th five-year plan, CASHIPS (KP-2017-16), National Key R&D Program of China (No. 2017YFA0207302) and Innovative Program of Development Foundation of Hefei Center for Physical Science and Technology (2017FXCX002) for financial support. The calculations in this paper have been conducted on the supercomputing system of USTC.

Conflict of interest

The authors declare no conflict of interest.

Keywords: Au nanoclusters · Au₄₂(TBBT)₂₆ · kernel-atom packing · photoluminescence · structural isomerism

How to cite: *Angew. Chem. Int. Ed.* **2019**, *58*, 4510–4514
Angew. Chem. **2019**, *131*, 4558–4562

- [1] a) O. Guliamov, L. Kronik, K. A. Jackson, *J. Chem. Phys.* **2005**, *123*, 204312; b) M. Ji, X. Gu, X. Li, X. Gong, J. Li, L.-S. Wang, *Angew. Chem. Int. Ed.* **2005**, *44*, 7119–7123; *Angew. Chem.* **2005**, *117*, 7281–7285; c) A. Lechtken, D. Schooss, J. R. Stairs, M. N. Blom, F. Furche, N. Morgner, O. Kostko, B. von Issendorff, M. M. Kappes, *Angew. Chem. Int. Ed.* **2007**, *46*, 2944–2948; *Angew. Chem.* **2007**, *119*, 3002–3006; d) W. Huang, R. Pal, L.-M. Wang, X. C. Zeng, L.-S. Wang, *J. Chem. Phys.* **2010**, *132*, 054305.
- [2] a) S. Tian, Y.-Z. Li, M.-B. Li, J. Yuan, J. Yang, Z. Wu, R. Jin, *Nat. Commun.* **2015**, *6*, 8667; b) Y. Kamei, Y. Shichibu, K. Konishi, *Angew. Chem. Int. Ed.* **2011**, *50*, 7442–7445; *Angew. Chem.* **2011**, *123*, 7580–7583; c) Y. Chen, C. Liu, Q. Tang, C. Zeng, T. Higaki, A. Das, D.-e. Jiang, N. L. Rosi, R. Jin, *J. Am. Chem. Soc.* **2016**, *138*, 1482–1485; d) S. Zhuang, L. Liao, M.-B. Li, C. Yao, Y. Zhao, H. Dong, J. Li, H. Deng, L. Li, Z. Wu, *Nanoscale* **2017**, *9*, 14809–14813.
- [3] a) S. Knoppe, T. Buergi, *Acc. Chem. Res.* **2014**, *47*, 1318–1326; b) A. Mathew, T. Pradeep, *Part. Part. Syst. Charact.* **2014**, *31*, 1017–1053; c) P. Yu, X. M. Wen, Y. R. Toh, X. Q. Ma, J. Tang, *Part. Part. Syst. Charact.* **2015**, *32*, 142–163; d) R. Jin, C. Zeng, M. Zhou, Y. Chen, *Chem. Rev.* **2016**, *116*, 10346–10413; e) I. Chakraborty, T. Pradeep, *Chem. Rev.* **2017**, *117*, 8208–8271; f) Q. Yao, T. Chen, X. Yuan, J. Xie, *Acc. Chem. Res.* **2018**, *51*, 1338–1348.
- [4] a) M. Zhu, S. Zhou, C. Yao, L. Liao, Z. Wu, *Nanoscale* **2014**, *6*, 14195–14199; b) C. P. Joshi, M. S. Bootharaju, M. J. Alhilaly, O. M. Bakr, *J. Am. Chem. Soc.* **2015**, *137*, 11578–11581; c) Y. Negishi, T. Nakazaki, S. Maloa, S. Takano, Y. Niihori, W. Kurashige, S. Yamazoe, T. Tsukuda, H. Hakkinen, *J. Am. Chem. Soc.* **2015**, *137*, 1206–1212; d) Y. Niihori, Y. Kikuchi, A. Kato, M. Matsuzaki, Y. Negishi, *ACS Nano* **2015**, *9*, 9347–9356; e) H. Dong, L. Liao, S. Zhuang, C. Yao, J. Chen, S. Tian, M. Zhu, X. Liu, L. Li, Z. Wu, *Nanoscale* **2017**, *9*, 3742–3746; f) L. Liao, S. Zhuang, P. Wang, Y. Xu, N. Yan, H. Dong, C. Wang, Y. Zhao, N. Xia, J. Li, H. Deng, Y. Pei, S.-K. Tian, Z. Wu, *Angew. Chem. Int. Ed.* **2017**, *56*, 12644–12648; *Angew. Chem.* **2017**, *129*, 12818–12822.
- [5] a) P. D. Jadzinsky, G. Calero, C. J. Ackerson, D. A. Bushnell, R. D. Kornberg, *Science* **2007**, *318*, 430–433; b) M. Zhu, C. M. Aikens, F. J. Hollander, G. C. Schatz, R. Jin, *J. Am. Chem. Soc.* **2008**, *130*, 5883–5885; c) M. W. Heaven, A. Dass, P. S. White, K. M. Holt, R. W. Murray, *J. Am. Chem. Soc.* **2008**, *130*, 3754–3755; d) C. L. Heinecke, T. W. Ni, S. Malola, V. Mäkinen, O. A. Wong, H. Häkkinen, C. J. Ackerson, *J. Am. Chem. Soc.* **2012**, *134*, 13316–13322; e) A. Desireddy, B. E. Conn, J. Guo, B. Yoon, R. N. Barnett, B. M. Monahan, K. Kirschbaum, W. P. Griffith, R. L. Whetten, U. Landman, T. P. Bigioni, *Nature* **2013**, *501*, 399–402; f) L. Liao, S. Zhuang, C. Yao, N. Yan, J. Chen, C. Wang, N. Xia, X. Liu, M.-B. Li, L. Li, X. Bao, Z. Wu, *J. Am. Chem. Soc.* **2016**, *138*, 10425–10428; g) C. Zeng, Y. Chen, K. Kirschbaum, K. J. Lambright, R. Jin, *Science* **2016**, *354*, 1580–1584; h) S. Antonello, T. Dainese, F. Pan, K. Rissanen, F. Maran, *J. Am. Chem. Soc.* **2017**, *139*, 4168–4174; i) G. Deng, S. Malola, J. Yan, Y. Han, P. Yuan, C. Zhao, X. Yuan, S. Lin, Z. Tang, B. K. Teo, H. Häkkinen, N. Zheng, *Angew. Chem. Int. Ed.* **2018**, *57*, 3421–3425; *Angew. Chem.* **2018**, *130*, 3479–3483; j) X.-K. Wan, Z.-J. Guan, Q.-M. Wang, *Angew. Chem. Int. Ed.* **2017**, *56*, 11494–11497; *Angew. Chem.* **2017**, *129*, 11652–11655; k) X. Liu, J. Chen, J. Yuan, Y. Li, J. Li, S. Zhou, C. Yao, L. Liao, S. Zhuang, Y. Zhao, H. Deng, J. Yang, Z. Wu, *Angew. Chem. Int. Ed.* **2018**, *57*, 11273–11277; *Angew. Chem.* **2018**, *130*, 11443–11447; l) S. Li, Z.-Y. Wang, G.-G. Gao, B. Li, P. Luo, Y.-J. Kong, H. Liu, S.-Q. Zang, *Angew. Chem. Int. Ed.* **2018**, *57*, 12775–12779; *Angew. Chem.* **2018**, *130*, 12957–12961; m) S.-S. Zhang, L. Feng, R. D. Senanayake, C. M. Aikens, X.-P. Wang, Q.-Q. Zhao, C.-H. Tung, D. Sun, *Chem. Sci.* **2018**, *9*, 1251–1258.
- [6] a) K. Kwak, Q. Tang, M. Kim, D.-e. Jiang, D. Lee, *J. Am. Chem. Soc.* **2015**, *137*, 10833–10840; b) W. Du, S. Jin, L. Xiong, M. Chen, J. Zhang, X. Zou, Y. Pei, S. Wang, M. Zhu, *J. Am. Chem. Soc.* **2017**, *139*, 1618–1624.
- [7] a) C. Zeng, H. Qian, T. Li, G. Li, N. L. Rosi, B. Yoon, R. N. Barnett, R. L. Whetten, U. Landman, R. Jin, *Angew. Chem. Int. Ed.* **2012**, *51*, 13114–13118; *Angew. Chem.* **2012**, *124*, 13291–13295; b) C. Zeng, T. Li, A. Das, N. L. Rosi, R. Jin, *J. Am. Chem. Soc.* **2013**, *135*, 10011–10013; c) C. Zeng, Y. Chen, C. Liu, K. Nobusada, N. L. Rosi, R. Jin, *Sci. Adv.* **2015**, *1*, e1500425; d) C. Zeng, Y. Chen, K. Iida, K. Nobusada, K. Kirschbaum, K. J. Lambright, R. Jin, *J. Am. Chem. Soc.* **2016**, *138*, 3950–3953; e) C. Zeng, C. Liu, Y. Chen, N. L. Rosi, R. Jin, *J. Am. Chem. Soc.* **2016**, *138*, 8710–8713; f) L. Liao, J. Chen, C. Wang, S. Zhuang, N. Yan, C. Yao, N. Xia, L. Li, X. Bao, Z. Wu, *Chem. Commun.* **2016**, *52*, 12036–12039; g) H. Dong, L. Liao, Z. Wu, *J. Phys. Chem. Lett.* **2017**, *8*, 5338–5343; h) S. Zhuang, L. Liao, Y. Zhao, J. Yuan, C. Yao, X. Liu, J. Li, H. Deng, J. Yang, Z. Wu, *Chem. Sci.* **2018**, *9*, 2437–2442.
- [8] H. Qian, W. T. Eckenhoff, Y. Zhu, T. Pintauer, R. Jin, *J. Am. Chem. Soc.* **2010**, *132*, 8280–8281.
- [9] a) Z. Gan, J. Chen, J. Wang, C. Wang, M.-B. Li, C. Yao, S. Zhuang, A. Xu, L. Li, Z. Wu, *Nat. Commun.* **2017**, *8*, 14739; b) N. Goswami, Q. Yao, Z. Luo, J. Li, T. Chen, J. Xie, *J. Phys. Chem. Lett.* **2016**, *7*, 962–975; c) M. Sugiuchi, J. Maeba, N. Okubo, M. Iwamura, K. Nozaki, K. Konishi, *J. Am. Chem. Soc.* **2017**, *139*, 17731–17734.
- [10] Z. Wu, R. Jin, *Nano Lett.* **2010**, *10*, 2568–2573.
- [11] a) Y. Yu, Z. Luo, D. M. Chevrier, D. T. Leong, P. Zhang, D.-e. Jiang, J. Xie, *J. Am. Chem. Soc.* **2014**, *136*, 1246–1249; b) Z. Gan, Y. Lin, L. Luo, G. Han, W. Liu, Z. Liu, C. Yao, L. Weng, L. Liao, J. Chen, X. Liu, Y. Luo, C. Wang, S. Wei, Z. Wu, *Angew. Chem.*

- Int. Ed.* **2016**, *55*, 11567–11571; *Angew. Chem.* **2016**, *128*, 11739–11743.
- [12] a) Z. Wu, M. A. MacDonald, J. Chen, P. Zhang, R. Jin, *J. Am. Chem. Soc.* **2011**, *133*, 9670–9673; b) X. Yuan, B. Zhang, Z. Luo, Q. Yao, D. T. Leong, N. Yan, J. Xie, *Angew. Chem. Int. Ed.* **2014**, *53*, 4623–4627; *Angew. Chem.* **2014**, *126*, 4711–4715.
- [13] S. Zhuang, L. Liao, J. Yuan, C. Wang, Y. Zhao, N. Xia, Z. Gan, W. Gu, J. Li, H. Deng, J. Yang, Z. Wu, *Angew. Chem. Int. Ed.* **2018**, *57*, 15450–15454; *Angew. Chem.* **2018**, *130*, 15676–15680.

Manuscript received: November 24, 2018
Accepted manuscript online: February 5, 2019
Version of record online: February 20, 2019